Pharmaceutical Research, Vol. 25, No. 8, August 2008 (© 2008)
DOI: 10.1007/s11095-008-9604-5

Research Paper

Intravital Microscopic Analysis of Vascular Perfusion and Macromolecule Extravasation after Photodynamic Vascular Targeting Therapy

Chong He,[1] Priyanka Agharkar,[1] and Bin Chen[1,2,3]

Received February 25, 2008; accepted April 16, 2008; published online April 30, 2008

Purpose. Photodynamic therapy (PDT), involving the combination of a photosensitizer and light, is being evaluated as a vascular disrupting therapy and drug delivery enhancement modality based on its effects on vascular perfusion and barrier function. Since tumor vasculature is the common route for the delivery of both blood and therapeutic agents, it is important to compare the effects of PDT on blood perfusion and substance transport.
Materials and Methods. Tumor blood cell velocity and the extravasation of high molecular weight dextran molecules were continuously monitored by intravital fluorescence microscopy for up to 60 min after PDT using three doses of verteporfin in the MatLyLu prostate tumor model.
Results. PDT induced tumor perfusion disruption via thrombus formation. PDT using a higher dose of verteporfin was more effective in inhibiting blood perfusion while a lower dose verteporfin-PDT was more potent in enhancing dextran extravasation. The increase in dextran extravasation induced by PDT was dependent upon dextran molecular weight. A lower molecular weight dextran obtained a higher tumor accumulation after PDT than a higher molecular weight dextran.
Conclusions. PDT with verteporfin had different effects on tumor vascular perfusion *versus* the extravasation of macromolecules. Optimal PDT conditions should be adjusted based on the therapeutic application.

KEY WORDS: benzoporphyrin derivative (BPD); blood flow; drug delivery; photodynamic therapy (PDT); photosensitizer; vascular permeability; vascular targeting.

INTRODUCTION

Tumor vasculature represents an important target for cancer therapy due to the dependence of tumor cells on a functional blood supply for cell growth, and blood-borne therapeutic agents to get access to tumor tissues (1). On the one hand, tumor blood vessels can be targeted by antiangiogenic and vascular disrupting agents to inhibit tumor progression (2). On the other hand, tumor vascular function can be modified to enhance the delivery of anticancer agents to tumor tissues because tumor vasculature is one of the major physiological barriers for sufficient delivery of therapeutic agents to tumor tissues, especially for macromolecular agents (3). Thus, strategies aimed at specifically disrupting the endothelial barrier integrity are being developed to improve delivery of therapeutic agents to the tumor tissues (4).

Photodynamic therapy (PDT) is an established cancer treatment modality, which involves the combination of a photosensitizing compound, light with a wavelength matching the absorption of photosensitizer, and oxygen molecules (5). Upon absorption of light, photosensitizer molecules are activated from the ground state to the triplet state, which then react with oxygen and produce highly reactive singlet oxygen. The mechanism of PDT is complicated, involving a combined effect of photocytotoxicity, vascular damage and immune reactions (6). Photodynamic vascular targeting therapy aims to selectively target tumor vasculature for therapeutic purposes. In this case, laser light is usually delivered to tumor tissues shortly after systematic administration of a photosensitizer when the drug is predominately localized within blood vessels (7). Preferential photosensitization of vascular components leads to vessel functional changes. This vascular-targeting modality has been approved for the treatment of age-related macular degeneration and is currently under clinical trial for prostate cancer treatment (7).

It was recently reported that PDT can be used to facilitate the delivery of macromolecular agents to tumor tissues via induced vascular leakage (8). We demonstrated in the MatLyLu rat prostate tumor model that vascular-targeting PDT with photosensitizer verteporfin significantly increases vascular permeability and tumor accumulation of circulating molecules (9). However, the same treatment was also found to cause vascular shutdown by inducing thrombus formation, resulting in extensive tumor necrosis. Because tumor vasculature is the common route for the delivery of both blood and therapeutic agents, it is important to understand how

[1] Department of Pharmaceutical Sciences, Philadelphia College of Pharmacy, University of the Sciences in Philadelphia, 600 South 43rd Street, Philadelphia, Pennsylvania 19104, USA.
[2] Department of Radiation Oncology, University of Pennsylvania, Philadelphia, Pennsylvania 19104, USA.
[3] To whom correspondence should be addressed. (e-mail: b.chen@usp.edu)

differently vascular-targeting PDT affects tumor perfusion and vascular barrier functions. Such knowledge is crucial to apply this modality for tumor targeting and anticancer drug delivery enhancement. By permitting high resolution imaging of vessel structure and function in live animals, intravital microscopy offers a powerful tool to study vascular morphology and function (10). Here we used this system to examine changes of vessel perfusion and barrier function after verteporfin-PDT targeting tumor blood vessels in an orthotopic rat prostate tumor model.

MATERIALS AND METHODS

Orthotopic Prostate Tumor Model. The orthotopic R3327-MatLyLu Dunning rat prostate tumor model was used in this study. The MatLyLu tumor is an androgen-independent prostate carcinoma, syngeneic to the male Copenhagen rats, and highly metastatic to lymph nodes and lungs (MatLyLu) (11). The MatLyLu cells were maintained in the RPMI-1640 with glutamine (Mediatech, Herndon, VA) supplemented with 10% fetal bovine serum (HyClone, Logan, UT) and 100 units/ml penicillin-streptomycin (Mediatech) at 37°C in a 5% CO_2 incubator. The orthotopic tumors were induced by injecting 1×10^5 tumor cells in the ventral lobe of prostate in the Copenhagen rats (6–8 weeks old, Charles River Laboratories, Wilmington, MA), as described previously (12). Tumors were used for experiments at 7–8 days after implantation with a size of 8–10 mm in diameter. All animal procedures were carried out according to the NIH Principles of Laboratory Animal Care and approved by the Institutional Animal Care and Use Committee (IACUC).

Photosensitizer. Verteporfin (benzoporphyrin derivative (BPD) monoacid ring A in a lipid-formulation) was obtained from QLT Inc. (Vancouver, Canada) as a gift. A stock saline solution of verteporfin was reconstituted according to the manufacturer's instruction and stored at 4°C in the dark. Stock solution of BPD was diluted right before injection.

PDT Treatments. A diode laser system (High Power Devices Inc., North Brunswick, NJ) with 690 nm wavelength was used for the irradiation of MatLyLu tumors. The laser was coupled to an optical fiber with 600 μm core diameter for light delivery. A microlens was connected to the end of fiber to achieve homogeneous irradiation of a 12 mm-diameter spot. The MatLyLu tumors were surgically exposed to illumination with an irradiance of 50 mW/cm^2 for 1,000 s, resulting in a total light dose of 50 J/cm^2. Light intensity was measured with an optical power meter (Thorlabs Inc, North Newton, NJ). Animals were anesthetized with injection (i.p.) of a mixture of ketamine (90 mg/kg) and xylazine (9 mg/kg) during treatment. Three different doses of verteporfin (0.25, 0.5 and 1.0 mg/kg) were examined, which was always i.v. injected at 15 min prior to light irradiation. We have shown in the previous study that verteporfin is primarily localized in the tumor vasculature at this time (13).

Intravital Fluorescence Microscopy. Immediately after PDT treatment, tumor-bearing animals were i.v. injected with 20 mg/kg of Hoechst, 5 mg/kg of fluorescein isothiocyanate-labeled dextran with a molecular weight of 2,000 kilo Dalton (2,000 kDa FITC-dextran), and 10 mg/kg of tetramethylrhodamine isothiocyanate-labeled dextran with a molecular weight of 155 kilo Dalton (155 kDa TRITC-dextran). These three fluorescence dyes (all from Sigma-Aldrich Corp, St. Louis, MO) were bolus injected as a mixture. The anesthetized animals were then placed in a prone position on the microscope stage and the MatLyLu tumors were imaged with a Leica DMI 6000B inverted fluorescence microscope. A microscopic field including clearly visible blood vessels was selected and imaged every 5 min for up to 60 min after injection. A 20× long working distance objective was used to image tumor tissues and different channel fluorescence images were captured with a Hamamatsu ORCA-AG CCD monochrome camera. The multi-channel image acquisition with appropriate filter setup was controlled by SimplePCI software (Compix Inc, Cranberry, PA). All the following image analyses were performed with the SimplePCI and NIH ImageJ software packages.

Analysis of Blood Cell Velocity. Blood cell flow velocity was measured based on the Hoechst channel (excitation: 360/40 nm; emission: 470/40 nm) images, which were captured at a speed of 17 frames per second for 3 s every 5 min after PDT. Hoechst dye stained the nuclei of circulating blood cells. Blood cell flow velocity was calculated by measuring the distance of Hoechst-positive cells traveled between two consecutive images divided by the time interval between these two images. Because the morphological differences between arteriols and venules in tumor tissues are often not distinct, vessels were chosen for velocity measurements solely based on the vessel size. In each animal, blood cell velocity values at different time points after PDT were normalized to the first point value, i.e. 5 min after PDT, to obtain the relative change after treatment. The percentage changes of each animal in the same group were pooled to generate an overall response curve.

Analysis of Blood Vessel Diameter and Fluorochrome-Labeled Dextran Extravasation. The FITC channel (excitation: 480/40 nm; emission: 527/30 nm) and TRITC channel (excitation: 546/12 nm; emission: 600/40 nm) images were captured every 5 min for up to 60 min after PDT with fixed camera settings. Images in each channel were properly oriented and stacked to ensure that measurements were taken at approximately the same location. Blood vessel diameter was measured based on the FITC-dextran images.

To measure the extravasation of fluorochrome-labeled dextrans in tumor tissues, regions of interest (ROIs) with diameter of 10 μm were selected on the FITC channel images. The same ROIs were also marked at same locations on the matched TRITC images. Although close to nearby blood vessels, these ROIs were chosen in areas without visible blood vessels. The average fluorescence intensity in ROIs was measured on the FITC and TRITC images taken at different times after PDT. All intensity values in each ROI were normalized to its first point value, i.e. 5 min after PDT, to obtain percentage changes as a function of time after treatment. Data of ROIs in the same group were pooled to generate the overall response curve. The area under curve (AUC) of each ROI intensity change curve was calculated to

represent the accumulation of fluorochrome-labeled dextran in tumor tissues over the 60 min period.

Statistical Analysis. Blood cell flow velocity, vessel diameter and fluorescence intensity data were first analyzed using repeated measures analysis of variance (ANOVA) with Tukey's post test to examine statistical differences among measurements taken at various time points during the 60 min period after treatment. One-way ANOVA test with Tukey's post test was then used to determine statistical differences between various treatment groups and the control group. Statistical significance was accepted at $p<0.05$. All statistical analyses were carried out using GraphPad Prism software (GraphPad, San Diego, CA).

RESULTS

Thrombus formation and blood flow stasis were two significant observations after PDT treatments. PDT with 0.25 mg/kg dose of verteporfin mainly induced the formation of emboli (unstable thrombi). Although reduction in blood flow was clearly visible, most blood vessels were still functional at the end of 60 min after this PDT treatment possibly due to the dislodging of unstable clots. As shown in Fig. 1, thrombus formation was observed as early as 5 min after 0.5 mg/kg dose of verteporfin-PDT. The development of thrombus caused vessel lumen narrowing and stagnant blood flow, resulting in complete perfusion arrest at 50 min after treatment.

Changes in blood cell flow velocity and vessel diameter were continuously measured for a period of 60 min after treatments and the data were shown in Fig. 2. There was a slight increase in blood cell velocity in control tumors, but this change was not statistically significant ($p>0.05$, Fig. 2A). PDT with 0.25 mg/kg dose of verteporfin induced up to 50% reduction in blood cell velocity after treatment ($p<0.01$). However, among eight blood vessels analyzed, six were still functional at the end of 60 min after PDT. Significant decrease in blood cell velocity was also observed in tumors treated with 0.5 mg/kg dose of verteporfin PDT ($p<0.01$). After a short rebound, blood cell velocity continued to decline to nearly complete perfusion arrest at 60 min after treatment. Only 2 out of 14 vessels analyzed were still functional at the end of observation. PDT with 1.0 mg/kg dose of verteporfin caused complete blood flow arrest within 20 min and no recovery was observed up to 60 min after PDT ($p<0.01$). Similar to control tumors, no significant change in vessel diameter was detected in tumors treated with either 0.25 or 0.5 mg/kg dose of verteporfin PDT ($p>0.05$, Fig. 2B). PDT with 1.0 mg/kg dose of verteporfin induced an initial vessel constriction followed by vessel dilation at late times. However, none of these changes were statistically significant compared to the 5 min time point ($p>0.05$).

Blood vessels analyzed in this study ranged from 0 to 1817.6 μm/s in blood cell velocity and from 8.3 to 83.1 μm in vessel diameter. There was no correlation between blood cell velocity and vessel diameter in control and all three PDT groups at any time point ($p>0.05$). As PDT with 0.5 mg/kg dose of verteporfin caused vascular shutdown in 12 out of 14 blood vessels observed within 60 min after PDT, we analyzed the relationship among vessel diameter, blood cell velocity and the time taken to reach zero blood flow. Figure 3 indicates no significant correlation between vessel diameter and blood cell velocity ($p=0.819$). Also there was no correlation between vessel diameter and the time taken to zero blood flow ($p=0.246$). However, a strong correlation was found between the initial blood cell velocity and the time taken to reach zero blood cell velocity ($p=0.007$).

Fluorescence images of 2,000 kDa FITC-dextran and 155 kDa TRITC-dextran were shown in Fig. 4 to illustrate the extravasation of macromolecules after treatments. Average fluorescence intensities of 2,000 kDa FITC-dextran and 155 kDa TRITC-dextran in ROIs were measured and shown

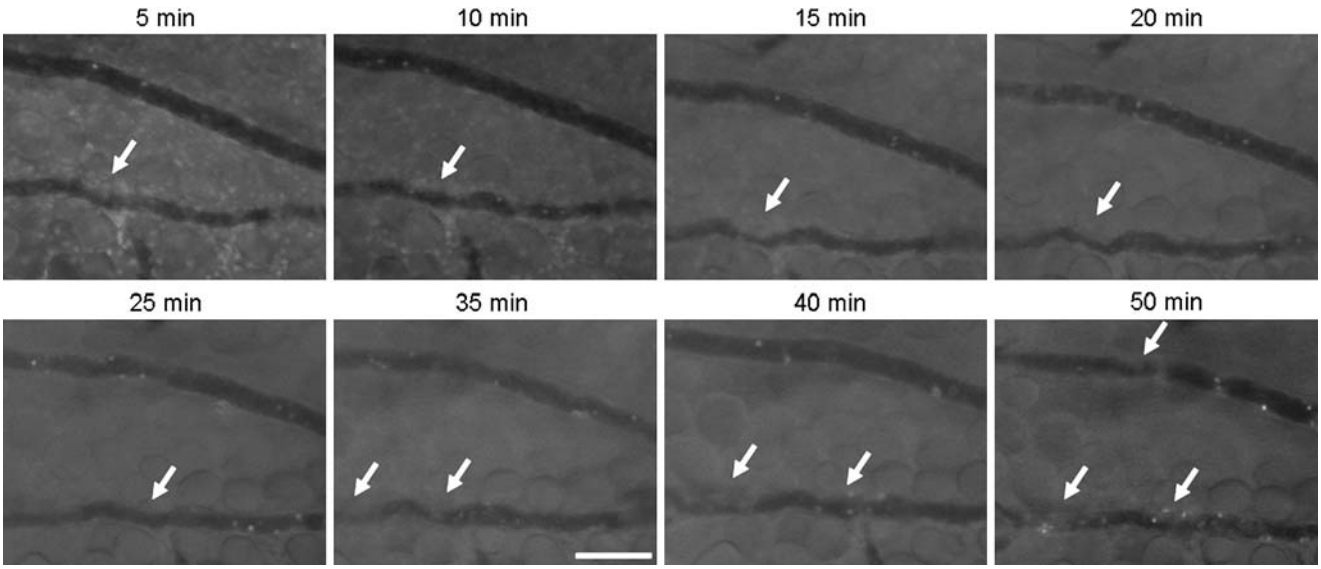

Fig. 1. Thrombus formation after PDT with verteporfin. The MatLyLu tumors were treated with 50 J/cm^2 light dose at 15 min after i.v. injection of 0.5 mg/kg dose of verteporfin. Tumor blood vessels were continuously imaged by intravital fluorescence microscopy showing the formation of thrombi (indicated by *arrows*) that caused progressive vessel lumen obstruction and ultimately vascular shutdown at 50 min after treatment. Bar=100 um.

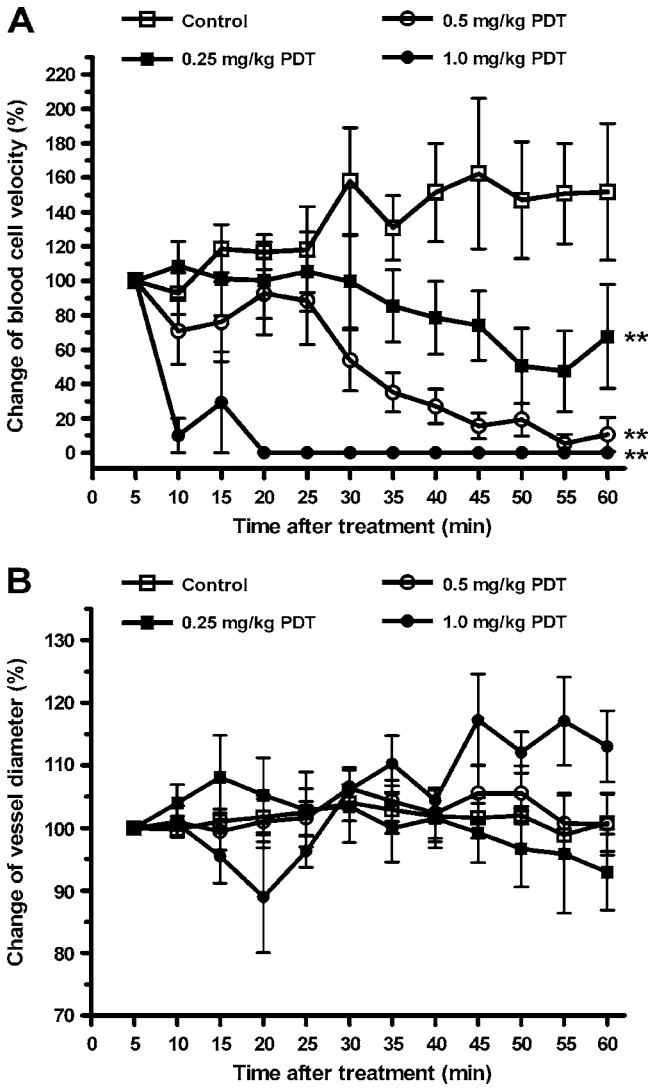

Fig. 2. Effects of PDT with verteporfin on blood cell velocity (**A**) and blood vessel diameter (**B**). The MatLyLu tumors were treated with 50 J/cm^2 light dose at 15 min after i.v. injection of 0.25, 0.5 or 1.0 mg/kg doses of verteporfin. Control tumors received no treatment. Blood cell velocity and vessel diameter were continuously measured every 5 min for up to 60 min after treatment by intravital fluorescence microscopy. Each data point represents the mean of 4–12 blood vessels and is expressed as a percentage of the 5 min point value. Bars indicate the standard error. Compared to the control, $^{**}p<0.01$.

in Fig. 5. The extravasation of 2,000 kDa FITC-dextran (Fig. 5A) and 155 kDa TRITC-dextran (Fig. 5B) led to significant increase in fluorescence intensity in untreated control tumors ($p<0.05$). Compared to untreated control tumors, PDT with 0.25 mg/kg dose of verteporfin significantly enhanced the extravasation of 2,000 kDa FITC-dextran in tumor tissues ($p<0.01$) while PDT with both 0.5 and 1.0 mg/kg doses of verteporfin had no significant effect on FITC-dextran extravasation ($p>0.05$). Both 0.25 and 0.5 mg/kg doses of verteporfin-PDT caused significant increase in the extravasation of 155 kDa TRITC-dextran compared to control tumors ($p<0.01$). But there was no significant difference between 0.25 and 0.5 mg/kg dose PDT treatments in affecting 155 kDa TRITC-dextran extravasation ($p>0.05$). PDT with 1.0 mg/kg dose of verteporfin induced an initial decrease in the fluorescence of 155 kDa TRITC-dextran. It is not clear what caused this decrease in the TRITC fluorescence, which was not observed in the corresponding FITC channel. The fluorescence of 155 kDa TRITC-dextran recovered after the initial decrease. Overall no significant difference was found between 1.0 mg/kg verteporfin-PDT and untreated control tumors in the TRITC-dextran extravasation over the 60 min period ($p>0.05$).

The AUC of fluorescence intensity–time curve was calculated to estimate tumor uptake of fluorochrome-labeled dextrans during the 60 min period (Fig. 6). Among three different doses of PDT treatments, only PDT with 0.25 mg/kg dose of verteporfin caused significant increase in tumor accumulation of 2,000 kDa FITC-dextran compared to control tumors ($p<0.05$). However, both 0.25 and 0.5 mg/kg doses of PDT significantly enhanced tumor accumulation of 155 kDa TRITC-dextran. Tumor uptake of 155 kDa TRITC-dextran was significantly higher than that of 2,000 kDa FITC-dextran after either 0.25 or 0.5 mg/kg PDT treatment ($p<0.01$). The 1.0 mg/kg dose PDT appeared to induce a decrease in tumor uptake of 155 kDa TRITC-dextran compared to control tumors, but this was not statistically significant ($p>0.05$).

DISCUSSION

Since tumor vasculature serves to provide blood supply to tumor tissues and regulate substance exchange between blood and tumor interstitial fluid (1), it is important to understand how a tumor vascular disrupting therapy affects these two key vascular functions. In the present study, we used intravital microscopy to analyze changes in tumor vascular perfusion and macromolecule extravasation after verteporfin-mediated photodynamic vascular targeting therapy in the orthotopic MatLyLu rat prostate tumor model. Based on our previous study that PDT with 0.25 mg/kg dose of verteporfin increases macromolecule extravasation and

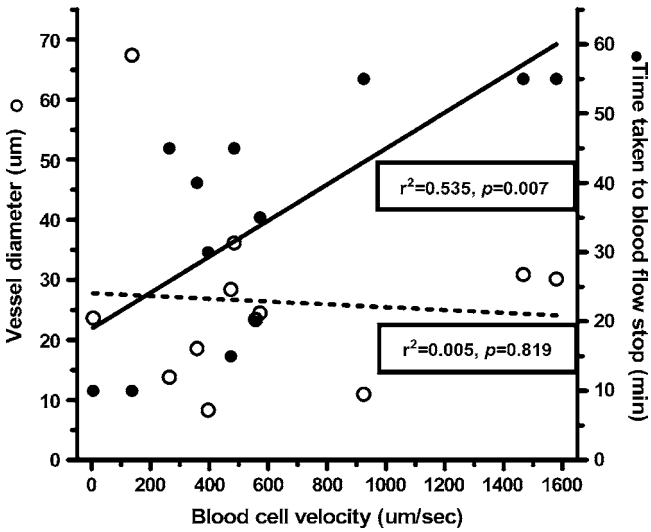

Fig. 3. Relationship between blood cell velocity and the time taken to reach zero blood flow after PDT with verteporfin. A significant correlation was found between the initial blood cell velocity and the time taken to zero blood cell velocity ($p=0.007$) after PDT with 0.5 mg/kg dose of verteporfin. The correlation between vessel diameter and blood cell velocity was not significant ($p=0.819$).

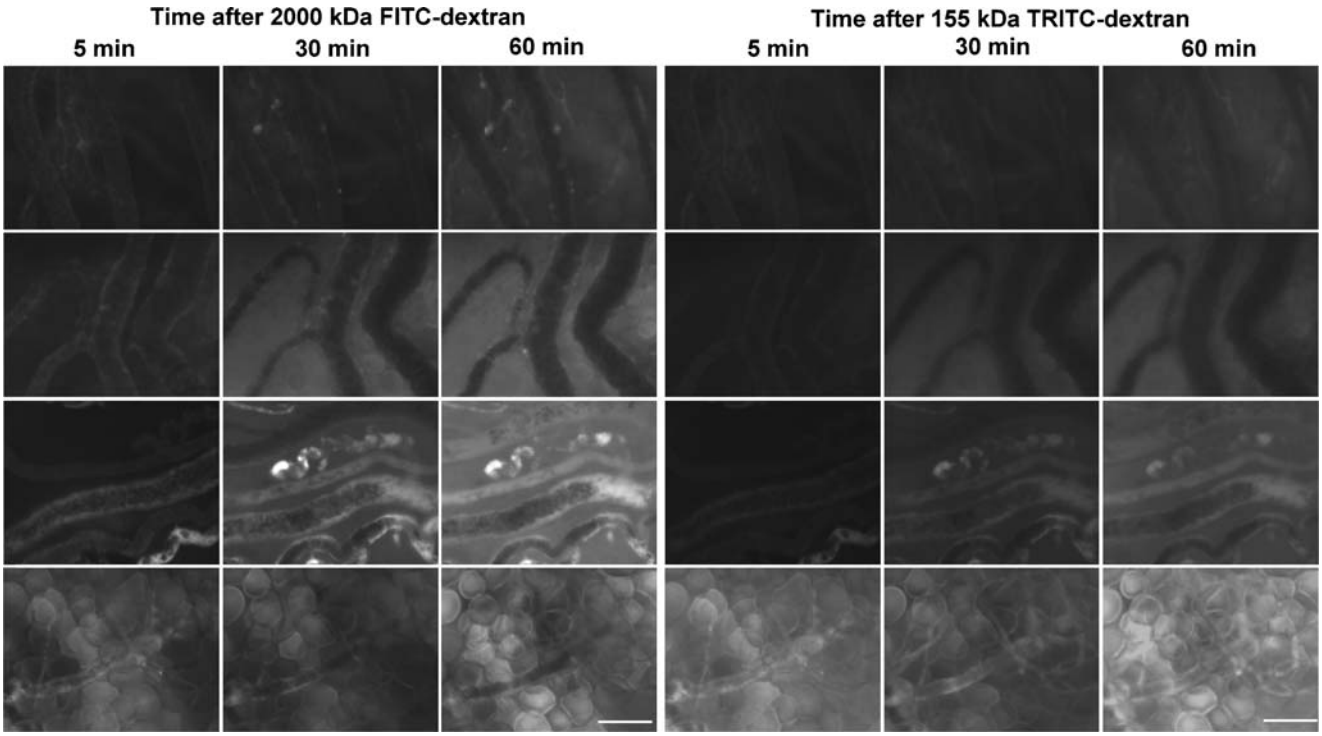

Fig. 4. Fluorescence images of 2,000 kDa FITC-dextran and 155 kDa TRITC-dextran at 5, 30 and 60 min after treatments. The MatLyLu tumors were treated with 50 J/cm^2 light dose at 15 min after i.v. injection of 0.25, 0.5 or 1.0 mg/kg doses of verteporfin. Control tumors received no treatment. Animals were i.v. injected with 2,000 kDa FITC-dextran and 155 kDa TRITC-dextran immediately after treatment and tumors were imaged with intravital fluorescence microcopy. *Top panel* control; *second panel* 0.25 mg/kg verteporfin-PDT; *third panel* 0.5 mg/kg verteporfin-PDT; *fourth panel* 1.0 mg/kg verteporfin-PDT. Bar=100 um.

induces tumor necrosis (9), we chose to examine two higher verteporfin doses (0.5 and 1.0 mg/kg) together with 0.25 mg/kg dose in this study. Our results demonstrate that PDT with verteporfin caused significant reduction in blood perfusion and an increase in the extravasation of dextran molecules. But the effects of PDT on blood perfusion and substance extravasation followed a reverse dose-dependence.

As expected, PDT with a higher dose of verteporfin was more effective in inducing blood flow reduction than a lower dose of verteporfin-PDT (Fig. 2). Similar to the previous studies (9,14,15), thrombus formation was found to contribute to PDT-induced vascular perfusion disruption. Stable thrombi formed inside vessel lumen caused blood flow reduction and even complete vascular occlusion. Even though vessel constriction was indeed observed in some blood vessels, vessel constriction in overall did not appear to play a major role in verteporfin-mediated vascular disruption, which has been reported to be involved in PDT with another photosensitizer Photofrin (16). Figure 2 indicates that no significant vessel size change was found after all three different doses of PDT treatments. This simply suggests the complexity of vessel response to PDT because, depending on the release of vasoactive substances with opposite effects on vessel size and spontaneous vessel response to tissue hypoxia, temperature and other microenvironment factors, both vessel constriction and dilation can happen at different time after verteporfin-PDT. These results are in agreement with those of Fingar *et al.* who reported that PDT with verteporfin had no significant effect on vessel diameter in a rat chondrosarcoma tumor model (15).

The mechanism underlying thrombus formation induced by photodynamic vascular targeting therapy is complicated and not yet clear. Reactive oxygen species generated intravascularly after PDT likely cause damage to multiple targets such as red blood cells, platelets and endothelial cells, which in turn leads to the activation of haemostatic cascades and results in thrombus formation (17,18). Endothelial damage plays an important role in initiating this cascade. As shown in the previous study, we have found a rapid endothelial cell microtubule depolymerization and endothelial cell contraction following verteporfin-PDT (9). Since endothelial cells form an interface between the blood and underneath tissue, these endothelial morphological changes lead to the exposure of tissue extracellular matrix to circulating blood, which causes blood cell adherence to the damaged endothelial cells via activating platelets and polymorphonuclear leukocytes (19,20). This might explain intravital microscopic observations that thrombi induced by verteporfin-PDT often started from endothelial sites and gradually increased in size, ultimately leading to blood vessel occlusion (Fig. 1).

Tumor blood vessels exhibited heterogeneity in response to PDT-induced perfusion disruption (21). By examining the response of each individual vessel to PDT, it is possible to identify the determinants that contribute to vascular response heterogeneity, which may help to find ways to enhance vascular response to PDT. Our data indicate that blood flow velocity was an important parameter in determining vascular response to PDT. Vessels with higher flow velocity were more resistant to PDT-induced vascular shutdown (Fig. 3). This is likely because high flow velocity was not conducive to

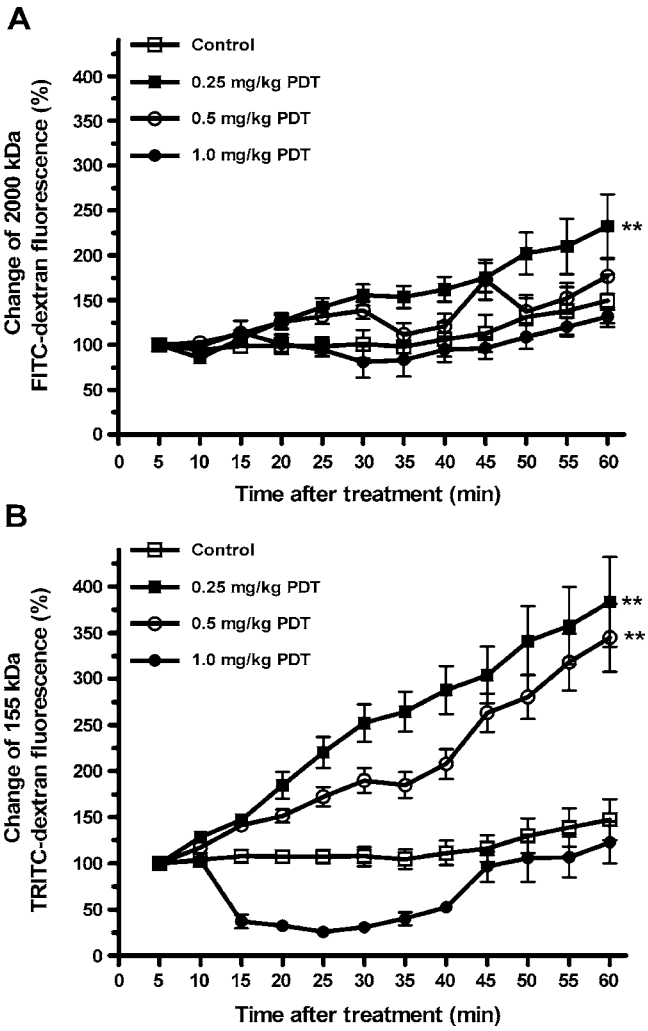

Fig. 5. Effects of PDT with verteporfin on the extravasation of 2,000 kDa FITC-dextran (**A**) and 155 kDa TRITC-dextran (**B**). The MatLyLu tumors were treated with 50 J/cm^2 light dose at 15 min after i.v. injection of 0.25, 0.5 or 1.0 mg/kg doses of verteporfin. Control tumors received no treatment. Animals were i.v. injected with 2,000 kDa FITC-dextran and 155 kDa TRITC-dextran immediately after treatment and tumors were imaged with intravital fluorescence microcopy. Fluorescence intensities of dextran molecules in the ROIs were continuously measured every 5 min for up to 60 min after treatment. Each data point represents the mean of 4–29 ROIs and is expressed as a percentage of the 5 min point value. *Bars* indicate the standard error. Compared to the control, $^{**}p<0.01$.

thrombus formation and able to push some already formed thrombi into circulation, which resumes blood perfusion function. Emboli were indeed commonly observed in blood vessels treated with a low dose of PDT and in vessels with fast blood flow in this study. A previous study demonstrates that tumor areas with low oxygen partial pressure (pO_2) have more rapid decrease in pO_2 level after verteporfin-PDT than areas with high pO_2 (22). Since it is very possible that tumor areas with low pO_2 also have low blood flow, the faster drop of tumor pO_2 in low pO_2 tumor areas than in high pO_2 tumor areas after PDT is likely because PDT induces a more rapid vascular shutdown in slow-flow vessels than in high-flow vessels. These results suggest that photodynamic vascular targeting therapy needs to be improved for targeting blood vessels with high blood flow. On the other hand, because tumor blood vessels generally have slower flow rate than normal vessels (23), this finding might explain why tumor vessels are more sensitive to vascular targeting PDT than normal vessels, which has been observed in the previous study (24).

Since vascular barrier is dependent upon endothelial tight junctions (25), another consequence of PDT-induced endothelial cell morphological change is the formation of inter-endothelial cell gaps, which disrupts vascular barrier. As shown in the present study, the extravasation and accumulation of high molecular weight dextran in tumor tissues were significantly increased as a result of vascular permeability increase after verteporfin-PDT. However, compared to the PDT effect on tumor perfusion, the effect of verteporfin-PDT on dextran delivery followed a reverse dose dependence. PDT with a lower dose of verteporfin was more effective in enhancing the extravasation and accumulation of dextran molecules in tumor tissues than a higher dose of verteporfin-PDT. This inverse dose dependence is likely due to the fact that PDT with a higher dose of verteporfin (e.g. 1.0 mg/kg) induced rapid vascular shutdown (Fig. 2), which prevented dextran molecules from being delivered to tumor tissues, while a lower dose verteporfin-PDT (e.g. 0.25 or 0.5 mg/kg) was able to maintain blood perfusion for sometime, which allowed continuous extravasation and accumulation of dextran molecules into the tumor tissue. These results suggest the importance of maintaining tumor perfusion in drug delivery enhancement by using a vascular targeted modality.

Our data also demonstrate that the enhancement of dextran delivery induced by verteporfin-PDT was dependent upon dextran molecular weight. Dextran with a lower molecular weight (155 kDa) exhibited a higher tumor extravasation and uptake than a higher molecular weight dextran (2,000 kDa) after both 0.25 and 0.5 mg/kg doses of PDT treatments. Since it has been known that tumor vascular permeability (26) and the transport of molecules in tumor interstitial area (27) decrease with the increase of molecular weight, the limited enhancement seen in the delivery of 2,000 kDa dextran was likely because it has a lower vascular permeability and slower diffusion in tumor interstitial area than the 155 kDa dextran.

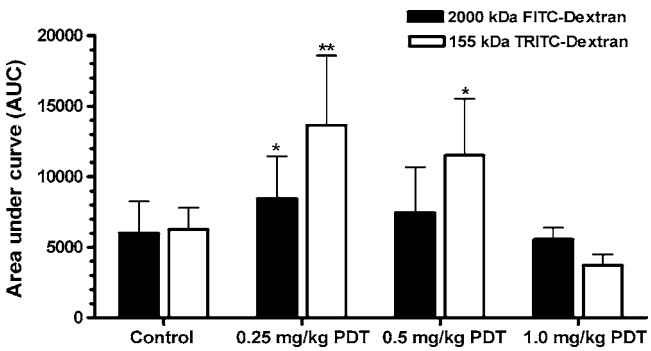

Fig. 6. Effects of PDT with verteporfin on the accumulation of 2,000 kDa FITC-dextran and 155 kDa TRITC-dextran in tumor tissues. The AUC of fluorescence intensity-time curve, as described in the legend of Fig. 5, was calculated to represent the tumor accumulation of dextran molecules. Compared to the control, $^{*}p<0.05$, $^{**}p<0.01$.

This study implies that, although photodynamic vascular targeting therapy with verteporfin may be used for both tumor destruction and drug delivery enhancement, optimal PDT conditions should be tailored to different therapeutic applications. PDT with a higher dose of verteporfin (e.g. 1.0 mg/kg) might be more appropriate for tumor eradication as a rapid and extensive vascular shutdown might be able to maximize tumor cell killing by oxygen and nutrients deprivation. We have found that PDT with 0.25 mg/kg dose of verteporfin causes substantial tumor necrosis. It remains to be determined whether PDT with a higher dose of verteporfin will lead to more tumor necrosis. For primarily enhancing the delivery of other therapeutic agents, PDT with a lower dose of verteporfin (e.g. 0.25 mg/kg) is likely preferred because it can obtain optimal drug tumor accumulation by maintaining tumor perfusion after treatment, as shown in the present and previous (9) study. PDT has been proposed to enhance the delivery of anticancer agent (8). Strategies such as illumination with low light doses and low dose rates (8) or in combination with anti-coagulants (28) also work through preserving tumor perfusion to obtain an enhanced drug delivery to tumor tissues. However, for most cancer combination therapies, PDT with an intermediate dose of verteporfin (e.g. 0.5 mg/kg) is likely to be a practical choice because this treatment can cause considerable tumor perfusion disruption and some effect of drug delivery enhancement, as demonstrated in the present study. Combination of intermediate dose PDT with anticancer drug therapy is more likely to achieve synergistic effect.

In conclusion, we found that photodynamic vascular targeting with verteporfin disrupted tumor perfusion by inducing thrombus formation, and enhanced tumor accumulation of high molecular weight dextrans by increasing vascular permeability. However, effects of PDT on blood perfusion and accumulation of dextran molecules followed a reverse dose dependence. A higher dose of verteporfin PDT was more effective in inducing perfusion disruption, but less effective in enhancing dextran accumulation. A lower dose of verteporfin PDT was favorable for drug delivery enhancement by maintaining tumor perfusion. Dextran with a lower molecular weight (155 kDa) obtained a higher tumor accumulation than a higher molecular weight dextran (2,000 kDa). These findings are important for optimizing PDT conditions as a vascular disrupting therapy or a modality for drug delivery enhancement.

ACKNOWLEDGEMENTS

This work is supported by Department of Defense (DOD) Grant W81XWH-06-1-0148 and Lindback Foundation. The authors would like to gratefully acknowledge Dr. Brian Pogue for reading the manuscript and QLT Inc. for providing photosensitizer verteporfin.

REFERENCES

1. C. Bouzin and O. Feron. Targeting tumor stroma and exploiting mature tumor vasculature to improve anti-cancer drug delivery. *Drug Resist. Updat.* **10**:109–20 (2007).
2. D. W. Siemann, M. C. Bibby, G. G. Dark, A. P. Dicker, F. A. Eskens, M. R. Horsman, D. Marme, and P. M. Lorusso. Differentiation and definition of vascular-targeted therapies. *Clin. Cancer Res*. **11**:416–20 (2005).
3. F. Yuan. Transvascular drug delivery in solid tumors. *Semin. Radiat. Oncol*. **8**:164–75 (1998).
4. G. P. van Nieuw Amerongen and V. W. van Hinsbergh. Targets for pharmacological intervention of endothelial hyperpermeability and barrier function. *Vasc. Pharmacol*. **39**:257–72 (2002).
5. T. J. Dougherty, C. J. Gomer, B. W. Henderson, G. Jori, D. Kessel, M. Korbelik, J. Moan, and Q. Peng. Photodynamic therapy. *J. Natl. Cancer Inst*. **90**:889–905 (1998).
6. D. E. Dolmans, D. Fukumura, and R. K. Jain. Photodynamic therapy for cancer. *Nat. Rev. Cancer.* **3**:380–7 (2003).
7. B. Chen, B. W. Pogue, P. J. Hoopes, and T. Hasan. Vascular and cellular targeting for photodynamic therapy. *Crit. Rev. Eukaryot Gene Expr.* **16**:279–305 (2006).
8. J. W. Snyder, W. R. Greco, D. A. Bellnier, L. Vaughan, and B. W. Henderson. Photodynamic therapy: a means to enhanced drug delivery to tumors. *Cancer Res*. **63**:8126–31 (2003).
9. B. Chen, B. W. Pogue, J. M. Luna, R. L. Hardman, P. J. Hoopes, and T. Hasan. Tumor vascular permeabilization by vascular-targeting photosensitization: effects, mechanism, and therapeutic implications. *Clin. Cancer Res*. **12**:917–23 (2006).
10. R. K. Jain, L. L. Munn, and D. Fukumura. Dissecting tumour pathophysiology using intravital microscopy. *Nat. Rev. Cancer* **2**:266–76 (2002).
11. T. R. Tennant, H. Kim, M. Sokoloff, and C. W. Rinker-Schaeffer. The Dunning model. *Prostate* **43**:295–302 (2000).
12. B. Chen, B. W. Pogue, X. Zhou, J. A. O'Hara, N. Solban, E. Demidenko, P. J. Hoopes, and T. Hasan. Effect of tumor host microenvironment on photodynamic therapy in a rat prostate tumor model. *Clin. Cancer Res*. **11**:720–7 (2005).
13. B. Chen, B. W. Pogue, P. J. Hoopes, and T. Hasan. Combining vascular and cellular targeting regimens enhances the efficacy of photodynamic therapy. *Int. J. Radiat. Oncol. Biol. Phys*. **61**:1216–26 (2005).
14. U. Schmidt-Erfurth and T. Hasan. Mechanisms of action of photodynamic therapy with verteporfin for the treatment of age-related macular degeneration. *Surv. Ophthalmol*. **45**:195–214 (2000).
15. V. H. Fingar, P. K. Kik, P. S. Haydon, P. B. Cerrito, M. Tseng, E. Abang, and T. J. Wieman. Analysis of acute vascular damage after photodynamic therapy using benzoporphyrin derivative (BPD). *Br. J. Cancer.* **79**:1702–8 (1999).
16. V. H. Fingar, T. J. Wieman, S. A. Wiehle, and P. B. Cerrito. The role of microvascular damage in photodynamic therapy: the effect of treatment on vessel constriction, permeability, and leukocyte adhesion. *Cancer Res*. **52**:4914–21 (1992).
17. V. H. Fingar. Vascular effects of photodynamic therapy. *J. Clin. Laser Med. Surg*. **14**:323–8 (1996).
18. B. Krammer. Vascular effects of photodynamic therapy. *Anticancer Res*. **21**:4271–7 (2001).
19. W. J. de Vree, M. C. Essers, H. S. de Bruijn, W. M. Star, J. F. Koster, and W. Sluiter. Evidence for an important role of neutrophils in the efficacy of photodynamic therapy *in vivo*. *Cancer Res*. **56**:2908–11 (1996).
20. W. J. de Vree, A. N. Fontijne-Dorsman, J. F. Koster, and W. Sluiter. Photodynamic treatment of human endothelial cells promotes the adherence of neutrophils *in vitro*. *Br. J. Cancer.* **73**:1335–40 (1996).
21. T. M. Busch. Local physiological changes during photodynamic therapy. *Lasers Surg. Med*. **38**:494–9 (2006).
22. B. W. Pogue, R. D. Braun, J. L. Lanzen, C. Erickson, and M. W. Dewhirst. Analysis of the heterogeneity of pO2 dynamics during photodynamic therapy with verteporfin. *Photochem. Photobiol.* **74**:700–6 (2001).
23. D. Fukumura and R. K. Jain. Tumor microenvironment abnormalities: causes, consequences, and strategies to normalize. *J. Cell Biochem*. **101**:937–49 (2007).
24. F. Borle, A. Radu, C. Fontolliet, H. van den Bergh, P. Monnier, and G. Wagnieres. Selectivity of the photosensitiser Tookad for photodynamic therapy evaluated in the Syrian golden hamster cheek pouch tumour model. *Br. J. Cancer.* **89**:2320–6 (2003).
25. G. Bazzoni. Endothelial tight junctions: permeable barriers of the vessel wall. *Thromb Haemost*. **95**:36–42 (2006).

26. M. R. Dreher, W. Liu, C. R. Michelich, M. W. Dewhirst, F. Yuan, and A. Chilkoti. Tumor vascular permeability, accumulation, and penetration of macromolecular drug carriers. *J. Natl. Cancer Inst.* **98**:335–44 (2006).
27. A. Pluen, Y. Boucher, S. Ramanujan, T. D. McKee, T. Gohongi, E. di Tomaso, E. B. Brown, Y. Izumi, R. B. Campbell, D. A. Berk, and R. K. Jain. Role of tumor–host interactions in interstitial diffusion of macromolecules: cranial *vs.* subcutaneous tumors. *Proc. Natl. Acad. Sci. U S A*. **98**:4628–33 (2001).
28. E. Debefve, B. Pegaz, J. P. Ballini, Y. N. Konan, and H. van den Bergh. Combination therapy using aspirin-enhanced photodynamic selective drug delivery. *Vasc. Pharmacol.* **46**:171–80 (2007).